

FORM FACTORS AND DIFFRACTIVE SCATTERING[†]

H. Moreno^{*} and R. Suaya^{**}

Stanford Linear Accelerator Center, Stanford University, Stanford, California 94305

ABSTRACT

Hadronic elastic and transition form factors are used to describe elastic nucleon-nucleon and pion-nucleon scattering, as well as diffractive excitation of nucleon resonances in an optical model. Very good quantitative agreement with available experimental results is obtained.

(Submitted to Phys. Letters B.)

† Work supported by the U. S. Atomic Energy Commission.

* Fellow of Centro de Investigación y de Estudios Avanzados del IPN and Consejo Nacional de Ciencia y Tecnología (México).

** Address after January 1, 1973: Depto. de Física, Universidad de Buenos Aires (Argentina).

High energy small angle pp scattering can give us a clue for the understanding of the diffractive mechanism in hadron-hadron collisions.

Recently, the Aachen-Cambridge-Genova-Torino collaboration¹ at CERN has measured the pp elastic differential cross section up to center of mass energies of 53 GeV and momentum transfers of -4 GeV^2 . Their preliminary results reported at the NAL conference show evidence of very little shrinkage (at least for $|t| > 0.1 \text{ GeV}^2$), and in addition, the shoulder structure seen at 20 GeV at $-t = 1.3 \text{ GeV}^2$ has developed into a clear dip at ISR energies.

Earlier measurements by the same group² of the differential cross section in the very forward direction show the presence of a kink around $-t = 0.1 \text{ GeV}^2$. This additional structure was parametrized with two exponentials. The quoted slope parameters at center of mass energy 53 GeV are $a = (12.4 \pm 0.3) \text{ GeV}^{-2}$ for $0.06 < -t < 0.11 \text{ GeV}^2$ and $a = (10.8 \pm 0.2) \text{ GeV}^{-2}$ for $0.168 < -t < 0.308 \text{ GeV}^2$.

Diffractive excitation of resonances (DER) in pp collisions has been recently measured³ at laboratory momentum up to 30 GeV/c. The common feature that these processes share with the elastic one is the absence of quantum number exchange in the t channel; namely, Pommeranchuk exchange. Nonetheless, if one compares the behavior of the differential cross section for the DER with the elastic, the following differences are encountered: (i) The forward slopes for the DER are consistently smaller than the elastic one (the 1400 Roper resonance is an exception to this rule). (ii) No evidence of a shoulder-like structure is seen up to the maximum momentum transfer measured, $-t \cong 6 \text{ GeV}^2$.

A variety of models⁴ have been proposed in order to understand the diffractive mechanism in pp scattering. In an attempt to explain the above

mentioned experimental results, we have considered the optical model as discussed by Chou and Yang⁵ for the elastic case. They propose the following form for the S matrix elements of elastic scattering at infinite energies for a given impact parameter b:

$$S(\vec{b}) = \exp[-A\rho(\vec{b})] , \quad (1)$$

where A is the absorption coefficient that may in general be complex, the matter density overlap, $\rho(\vec{b})$, is given by the two dimensional Fourier transform of the product of the hadronic matter form factors:

$$\rho(\vec{b}) = \frac{1}{2\pi} \int d^2k e^{i\vec{k}\cdot\vec{b}} G_1(k^2) G_2(k^2) . \quad (2)$$

The elastic scattering amplitude is given by:

$$f(t) = \frac{i}{2\pi} \int d^2b (1-S(\vec{b})) e^{-i\vec{q}\cdot\vec{b}} , \quad (3)$$

where $-t = \vec{q}^2$, and the following normalization is used:

$$\frac{d\sigma}{dt} = \pi |f(t)|^2 , \quad (4)$$

$$\sigma_T = 4\pi \text{Im} f(0) . \quad (5)$$

Following the standard lore, we will identify the matter distribution with the one measured electromagnetically. Assuming a power law behavior for the form factors

$$G(k^2) = \mu^{2p} (k^2 + \mu^2)^{-p} \quad (6)$$

leads to

$$\rho(\vec{b}) = \frac{\mu^2}{2^{2p-1} \Gamma(2p)} (\mu b)^{2p-1} K_{2p-1}(\mu b) , \quad (7)$$

if $G_1(k^2) = G_2(k^2)$, with $b = |\vec{b}|$, K_ν is the modified Bessel function of order ν .

The elastic pp scattering amplitude in the forward direction is taken to be purely imaginary, which is consistent with direct measurements of the real part by Coulomb interference techniques.⁶ This in turn implies that A as defined in Eq. (1) is real, and that its value is fixed by the total cross section, taken to be 40 mb. The resulting differential cross sections are completely specified by the knowledge of the form factors. If one utilizes the empirical dipole fit ($p=2$, $\mu^2 = 0.71$) excellent agreement with the experiment is obtained.² (See Figure 1.)

In Figure 1 we also plot the resulting cross sections when the power law fall-off of the input form factor is slightly modified ($p=2.2$, 1.9). The three cases so far analyzed present the common feature of developing a zero at approximately $t = -1.3 \text{ GeV}^2$. Additional zeroes, not shown in the figure, are present for larger $|t|$ values. For $p=2$ the second zero is at $|t| = 4.05 \text{ GeV}^2$, the second zero moves toward smaller values of $|t|$ as p increases. The height of the secondary maximum is also dependent on p .

The position of the zeroes also depend on the parameters μ^2 and A. Qualitatively, the following results emerge in this model: as A increases slightly (and hence the total cross section also increases) with μ^2 fixed, the position of the first zero moves inward. For constant A and increasing μ^2 , the zeroes move outward and the cross section falls. Finally for fixed total cross section, as μ^2 increases the first zero moves toward the origin and the distance between zeroes increases.

In the very forward direction the experimentally observed kink at $-t = 0.1 \text{ GeV}^2$ comes out quite naturally in this model⁸, and if the cross sections are parametrized as in reference 2, the results are as listed in Table I.

TABLE I

p	$a_1 \text{ GeV}^{-2} \quad (0 < -t < 0.1 \text{ GeV}^2)$	$a_2 \text{ GeV}^{-2} \quad (0.1 < -t < 0.2 \text{ GeV}^2)$
1.9	11.97	10.85
2.0	12.43	11.51
2.2	13.29	12.42

Encouraged by the successful description of pp elastic scattering, we have used this model to predict the behavior of pion-nucleon elastic scattering at asymptotic energies. Contrary to the pp case, we have very limited information on the behavior of the form factor of the pion. For simplicity we will consider only two choices for the pion form factor; i. e. simple pole $(-t + a^2)^{-1}$, and dipole $(-t + a^2)^{-2}$. The value of a^2 can be directly related to the mean square radius by the well-known formula $\langle r_\pi^2 \rangle = 6 G'(0)/G(0) = 6p/a^2$. Lacking good experimental determinations, we use as an input for the pion radius the theoretical bounds⁹ $(0.72 \pm 0.18) \text{ f} \leq r_\pi \leq (0.85 \pm 0.15) \text{ f}$. The resulting $\rho(b)$ are given by:

$$\rho(b)_{\text{simple pole}} = \frac{a^2 \mu^4}{(\mu^2 - a^2)^2} \left[\frac{K_0(ab) - K_0(\mu b)}{\mu^2 - a^2} - \frac{(\mu b) K_1(\mu b)}{2\mu^2} \right]; \quad (8)$$

$$\rho(b)_{\text{dipole}} = \frac{a^4 \mu^4}{(a^2 - \mu^2)^2} \left[\frac{(ab) K_1(ab)}{2a^2} + \frac{(\mu b) K_1(\mu b)}{2\mu^2} + \frac{2K_0(ab)}{a^2 - \mu^2} - \frac{2K_0(\mu b)}{a^2 - \mu^2} \right]; \quad (9)$$

where we have taken the dipole fit for the proton form factor and set $\mu^2 = 0.71$. In the special case when $\mu^2 = a^2$, Eqs. (8) and (9) have Eq. (7) as a limit. In Figure 2 we display the resulting predictions. The total pion-nucleon cross section was taken to be 24.2 mb.

It is interesting to notice that for simple pole pion form factors a smooth cross section is predicted at least up to $|t| = 6 \text{ GeV}^2$. On the other hand, for dipole form factors a dip starts to develop at $-t = 3.8 \text{ GeV}^2$ as one varies the value of the pion radius toward its lower limit 0.54 f. If the radius is equal to 0.535 f, a zero appears at this value of t , and if it is 0.53 f that zero splits into two, one located at $-t = 3.55 \text{ GeV}^2$ and the other at 4.05 GeV^2 .

Our results also show that clear deviations from a single exponential behavior should be present for $|t| < 0.4 \text{ GeV}^2$. Hopefully, these deviations will be seen at NAL energies. We find a kink in the cross section at $|t| \sim 0.1 \text{ GeV}^2$ and the predicted slope parameters are shown in Table II.

TABLE II

p	r_π [f]	a_1 [GeV ⁻²]	a_2 [GeV ⁻²]
		($-t < 0.1 \text{ GeV}^2$)	($0.1 < -t < 0.2 \text{ GeV}^2$)
1	0.86	11.90	10.11
	0.54	8.75	8.03
2	0.86	12.02	10.68
	0.54	8.75	8.03

It is clear that a realistic theory should include unitarity corrections to the simple optical picture, e. g. modify the simple ansatz given for $S(b)$. These corrections can be more easily visualized if one relies on the eikonal expansion. In this case the product of form factors represents the Born term (imaginary, corresponding to absorption) which is to be iterated in the multiple scattering series. Each term in the Glauber expansion has a simple diagrammatic correspondence¹⁰ and the series represents the sum of the Pomernanchuk contribution

plus all its associated cuts. Thus, in this context the DER should be included in the Glauber expansion. In particular, the number of channels that will shadow the elastic one will increase with energy. The whole picture becomes much more complicated and even the starting idea of exponentiation of the $S(b)$ may be lost. Investigations of this effect has been discussed in the literature.¹¹ In particular, as has been emphasized by Abarbanel, Drell and Gilman, if one replaced the complex "phase shift" $A\rho(b)$ in $S(b)$ by $\chi = 2 \tan^{-1}[A\rho(b)/2]$, in order to preserve the unitarity cut¹², the resulting dips of the optical model go away, in disagreement with experiment.

Due to the obvious difficulties associated with the multichannel formalism, its apparent shortcomings within simple models, and the success of the optical picture in its most commonly used form, we have not included the above described corrections, keeping in mind that the model's eventual agreement with experiment is what makes it palatable.

Going one step further in our degree of speculation, we have considered the DER, and we have approached the impact parameter representation of the amplitude $f_{tr}(t)$ for $pp \rightarrow pp^*$ in two different ways.

The first one corresponds to a bold generalization of the Chou-Yang idea. We take as an ansatz to replace $G_A(t) G_B(t)$ by $G_A(t) G_{p \rightarrow p^*}(t)$ in Eqs. (1-2), where $G_{p \rightarrow p^*}(t)$ represents the transition form factors.¹³

Elitzur¹⁴ has introduced the idea of scaling of the hadronic form factors, i. e. the excitation form factors are represented as functions of a single variable t/M^2 , M the resonance mass. A similar idea has proved to be useful in order to understand the observed scaling of the structure functions in deep inelastic electroproduction.¹⁵ We will therefore, parametrize $G_{p \rightarrow p^*}(t)$ as

$$G_{p \rightarrow p^*}(t) = (1 - t/\mu_i^2)^{-2} \tag{10}$$

$$\mu_i^2 = 0.71 M_i^2/m^2$$

where m is the proton mass, and restrict ourselves to the dipole form.

The resulting $\rho(b)$ coincides with ρ_{dipole} as given in Eq. (9) with a^2 replaced by μ_i^2 . The normalization used is:

$$\frac{d\sigma}{dt} \Big|_{\text{tr}} = \pi |f_{\text{tr}}(t)|^2 \tag{11}$$

with

$$f_{\text{tr}}(t) = i \int_0^\infty db b J_0(b\sqrt{-t}) S_{\text{tr}}(b) .$$

We have applied this prescription to the analysis of the two more prominent $I = \frac{1}{2}$ nucleon resonances $D_{13}(1520)$ and $F_{15}(1688)$. The parameter A in Eq. (1) was fixed requiring that the intercept at $t=0$ be given by 1 mb/GeV^2 and 2 mb/GeV^2 respectively. The t dependence of the $N(1520)$ and $N(1688)$ are very similar both theoretically and experimentally. The results of our calculation for the $N(1520)$ are shown in Figure 3. The agreement with experiments up to the maximum momentum transfer $|t| < 6 \text{ GeV}^2$ is remarkable. It must be stressed that, just as in the pp elastic case, our predictions do not depend on any arbitrary parameter. The agreement came as a surprise to us, considering that this model is supposed to be valid for small angles and asymptotic energies, and at 24 GeV/c energy dependent effects are expected to be important, as was observed for the elastic channel, and the t range covered includes large angle scattering as well.

Our second approach to DER is a simple attempt to incorporate multi-channel effects in our calculations, and for that purpose we have revisited the

distorted wave Born approximation.¹⁶ The resulting partial wave S-matrix elements can be approximated by

$$S_{\alpha\beta}^{\ell} \sim e^{i\delta_{\ell}^{\alpha}} B_{\alpha\beta}^{\ell} e^{i\delta_{\ell}^{\beta}} \quad (12)$$

where δ_{ℓ}^{α} and δ_{ℓ}^{β} represent the elastic phase shifts of the initial and final channels and $B_{\alpha\beta}^{\ell}$ is the Born transition matrix element. This kind of result has theoretical justification in the context of high energy potential scattering, where only two coupled channels are considered. Using the standard techniques valid at high energy, small angle scattering, we replace the discrete summation on ℓ by an integral over the continuous impact parameter b and arrive at:

$$f_{pp \rightarrow pp^*}(t) = iB \int_0^{\infty} b db J_0(b\sqrt{-t}) S_{el}^{(b)} \rho_{dipole}^{(b)} \quad (13)$$

where we have in addition assumed that the initial and final state elastic scattering are equal, and as before, we only consider the dipole form factor as input for $S_{el}^{(b)}$. By requiring that $\frac{d\sigma}{dt} \Big|_{t=0} = 1 \text{ mb/ GeV}^2$, B is fixed and there are no free parameters left.

The resulting prediction is also displayed in Figure 3 for comparison with the previous calculations, and the difference between the two results speaks for itself.

Summarizing, we have described diffractive scattering in terms of a simple model that has as input the matter form factors of the colliding particles. The excellent agreement we have obtained with experiment gives us ground to suspect that the physics behind the model is sound, but much theoretical and experimental work remains to be done to fully test the predictive power of this scheme. In particular, results of pion experiments at NAL are eagerly awaited.

Acknowledgement

Discussions with R. Blankenbecler, D. Broadhurst, and F. Gilman are appreciated. We would also like to thank J. Willemsen for a careful reading of the manuscript. One of us (HM) thanks the Centro de Investigación y de Estudios Avanzados del IPN and the Consejo Nacional de Ciencia y Tecnología of México for their financial support.

Footnotes and References

1. Report given by C. Rubbia at the XVI International Conference on High Energy Physics, Batavia, Illinois, September 6-13, 1972, unpublished.
2. G. Barbiellini et al., Phys. Letters 39B, 663 (1972).
3. J. V. Allaby et al., Report No. CERN-72-3132, submitted to Nuclear Phys. B, and references cited therein.
4. J. D. Jackson, Rev. Mod. Phys. 42, 12 (1970), and references quoted therein.
5. T. T. Chou and C. N. Yang, Phys. Rev. 170, 1591 (1968). See also L. Durand and R. Lipes, Phys. Rev. Letters 20, 637 (1968).
6. U. Amaldi et al., CERN preprint, September 1972, presented at the XVI International Conference on High Energy Physics, Batavia, Illinois, September 6-13, 1972, unpublished.
7. Durand and Lipes, loc. cit. have found that in order to fit the elastic cross section at 24 GeV/c instead of $\mu^2 = 0.71 \text{ GeV}^2$, $\mu^2 = 1 \text{ GeV}^2$ is favored. If, on the other hand, one uses the latter value of μ^2 to predict the cross section at $s = 2900 \text{ GeV}^2$ serious discrepancies with experiment arise, especially in the forward slopes and the secondary maximum that would turn out to be nearly two orders of magnitude above the data.
8. J. N. J. White, Report No. DNPL-P134, unpublished.
9. V. Z. Baluni, Teoret. and Matemat. Phizika 10, 19 (1972).
10. See J. D. Jackson, loc. cit.
11. H. D. I. Abarbanel, S. D. Drell and F. J. Gilman, Phys. Rev. 177, 2458 (1969). See also W. Drechsler and R. Suaya, Phys. Rev. D2, 1879 (1970).

12. R. Blankenbecler and M. L. Goldberger, Phys. Rev. 126, 766 (1962).
13. This particular ansatz for the S matrix elements, for a given impact parameter b : $\langle pp^* | S(b) | pp \rangle = \exp[-A\rho_{tr}(b)]$ is not to be understood in terms of a multiple scattering series, but rather as the matrix elements of a complicated operator.
14. M. Elitzur, Phys. Rev. Letters 27, 895 (1971).
15. E. D. Bloom and F. J. Gilman, Phys. Rev. D4, 2901 (1971).
G. Domokos, S. Kovesi-Domokos and E. Schonberg, Phys. Rev. D3, 1184 (1971). H. Moreno and J. Pestieau, Phys. Rev. D5, 1210 (1972).
16. L. Durand and Y. T. Chiu, Phys. Rev. 139B, 646 (1965). See also K. Gottfried and J. D. Jackson, Nuovo Cimento 34, 735 (1964).

Note Added

When this work was completed we received a preprint by M. Elitzur and R. Lipes (Carnegie-Mellon preprint, unpublished), where a similar idea is used to discuss pp scattering. These authors consider the multichannel problem as an effective 3-coupled channel one, and find, in agreement with our results, that unitarity corrections tend to spoil the uncorrected theoretical predictions.

Figure Captions

- Figure 1 Theoretical cross sections for pp elastic scattering. Curves A, B, C correspond to $p = 2.2, 2, 1.9$ and absorption coefficients $10.40, 9.90$ and 10.66 GeV^{-2} respectively. The preliminary experimental points of the Aachen-Cambridge-Genova-Torino collaboration at CERN for $E_{\text{cm}} = 53 \text{ GeV}$ are also displayed.
- Figure 2 Theoretical predictions for pion-nucleon elastic scattering. Curves A, D correspond to dipole pion form factor, pion radii of 0.54 and 1 f , and absorption coefficients 5.94 and 5.62 GeV^{-2} respectively. Curves C, B correspond to simple pole pion form factor, pion radii 0.54 and 1 f , and absorption coefficients 6.07 and 5.55 GeV^{-2} .
- Figure 3 Diffractive excitation of $N(1520)$. Curve A was calculated with an absorption coefficient equal to 0.93 GeV^{-2} . Curve B results from the absorbed Born approximation of Eq. (13). Also shown are the experimental points of Allaby et al. (1968) at $19.2 \text{ GeV}/c$, and of Allaby et al. (1972) at $24 \text{ GeV}/c$.

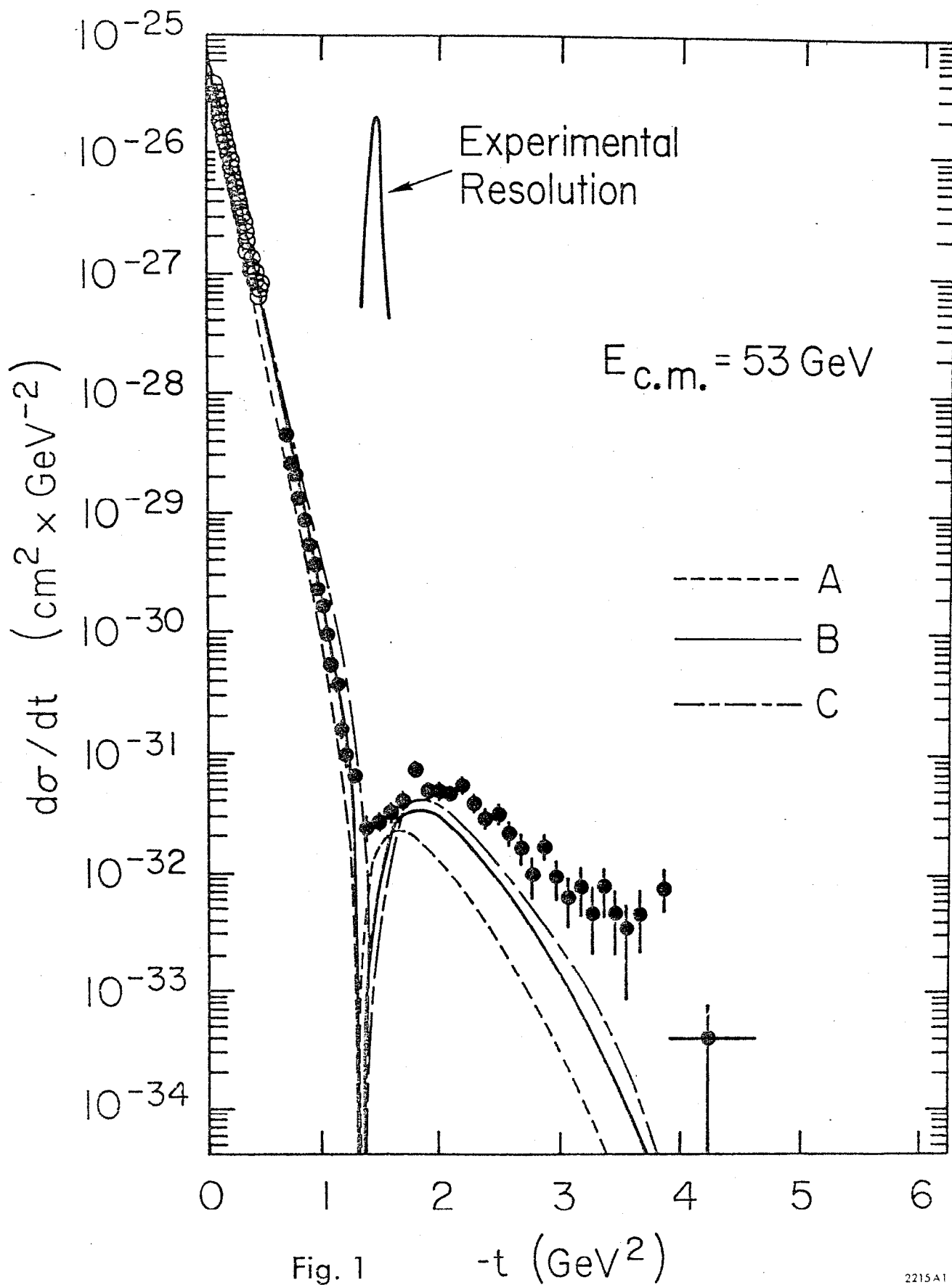


Fig. 1

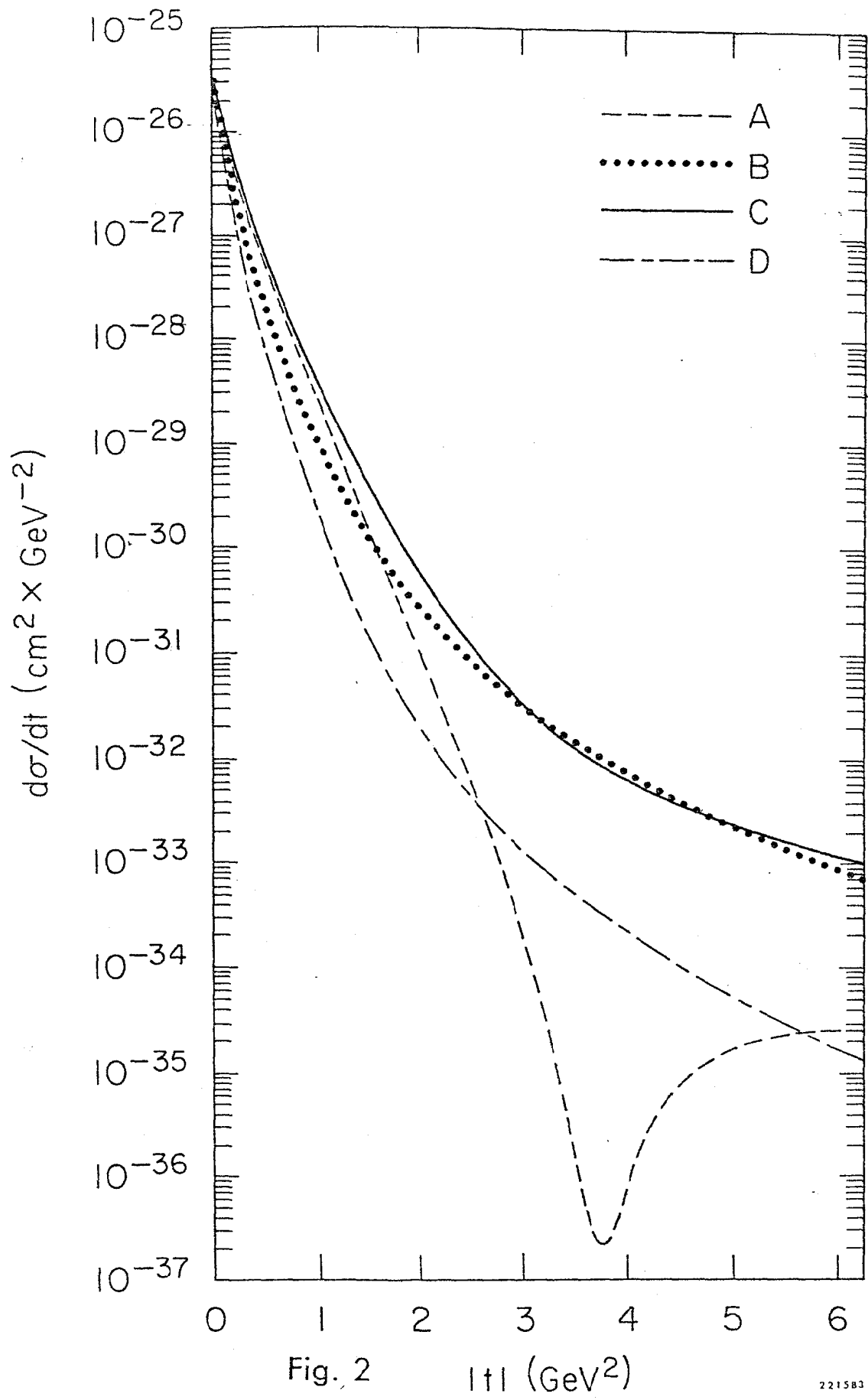


Fig. 2

$|t|$ (GeV^2)

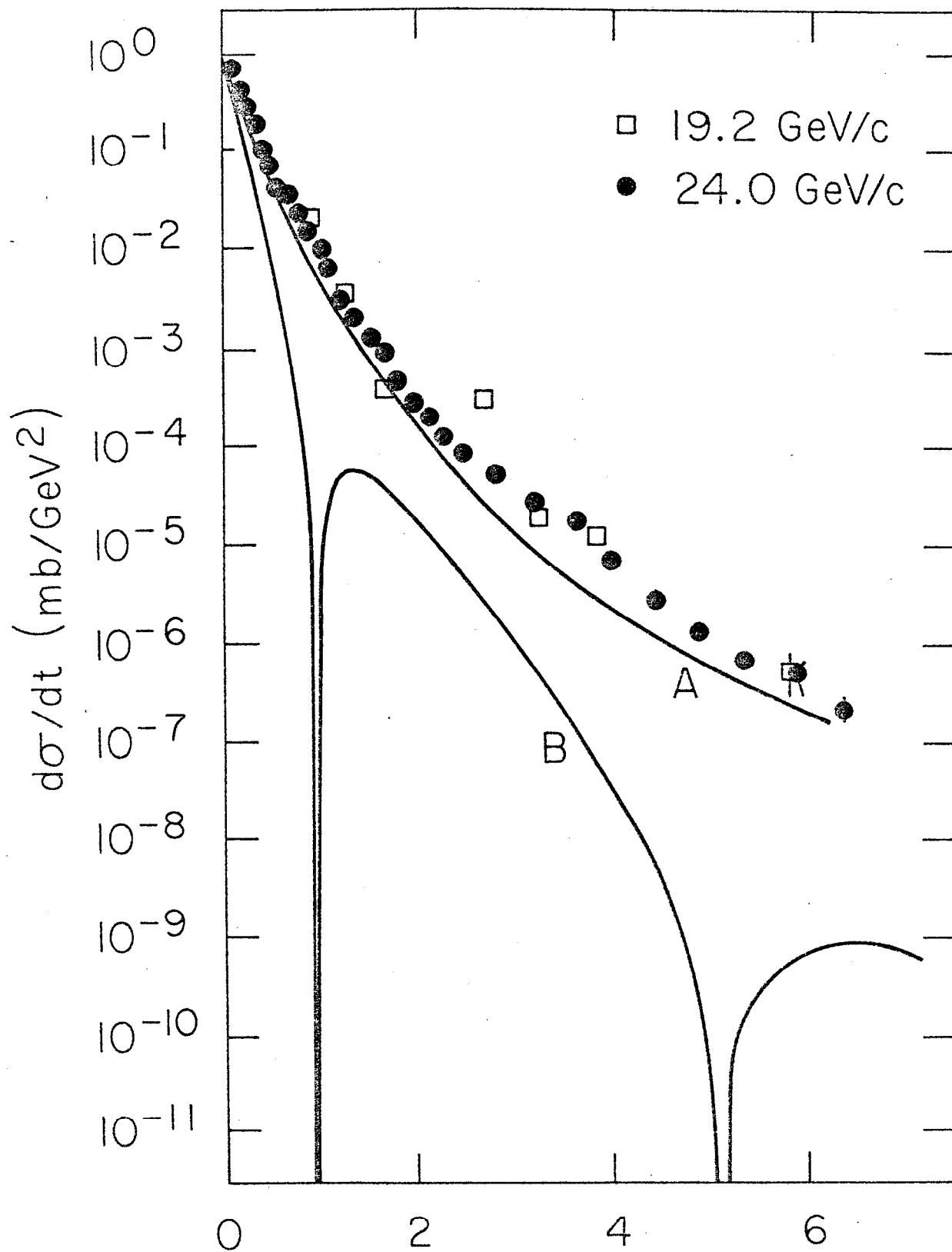


Fig. 3 FOUR MOMENTUM TRANSFER SQUARED, $|t|$ (GeV²)